J-integral, R-curve Testing of 5052 H112 Aluminum, Utilizing D.C. Potential Drop and Infrared Thermographic Methods

Y. HUANG*, G. E. HICHO** and R. J. FIELDS**

*Guest Researcher from the Institute of Metal Research, Academia Sinica, PRC

**National Institute of Standards and Technology, Metallurgy Division, Gaithersburg, Maryland 20899, USA

ABSTRACT

J-integral fracture toughness tests were performed at room temperature on aluminum three point bend and compact tension specimens. The ductile-crack-growth resistance curves were measured using the multi-specimen method. Crack growth was automatically recorded using the potential drop technique. Also an infrared vibro-thermographic technique was developed in order to measure crack initiation and propagation during unloading compliance determination. The initial parts of the J-R curves obtained were different for each method used, however for larger Δa_p values, the curves were essentially the same.

A continuous process of alternating crack-tip cooling and heating emissions, and ductile crack extension were observed from initiation to final fracture using measuring infrared apparatus. A novel vibro-thermographic technique made it possible to obtain real-time measurements of both crack initiation and extension during the entire fracture-toughness test.

KEY WORDS

Aluminum, DC potential drop, displacement, elastic-plastic fracture, fracture test, infrared crack extension recording, J-R curves, single-specimen compliance technique, thermograph.

INTRODUCTION

Critical J values for the onset of crack growth and J based on crack growth resistance curves are the most important parameters for elastic-plastic material characterization and ductile failure assessment. Besides the multiple-specimen method, as used in the ASTM E 813 for the determination of J_{IC}, a single-specimen procedure is available. This procedure forms the basis for an experimental test procedure for determining the material resistance curve where $J_R = J(\Delta a_p)$ (ASTM E-13, 1987).

For these methods, the crack driving parameter J is determined from the

force-displacement diagram. The methods differ in the way the increments of crack length are determined. Crack extension measurement, using the multiple specimen measurement involves the loading of specimens to selected different displacement levels and marking the amount of crack extension that occurred during each loading. In the single specimen method, a specimen is loaded to a predetermined load, and then unloaded to where a minor load remains. Crack extension can be measured by either by the unloading compliance or by the potential drop method.

There are two types of potential drop methods that could be used for crack measurements, one based on AC, the other DC (Hackett, et. al., 1983, Joyce, et. al., 1986). In this paper, results obtained using the change in electrical resistance (direct current potential drop - DCPD) method, and the elastic compliance (partial unloading compliance - PUC) method for stable crack growth evaluation were compared to the actual crack length measurements observed on the fracture surfaces of a series of specimens. Also an IR vibro-thermographic technique was developed and used to continuously measure crack tip position during elastic unloading compliance testing.

Results for IR vibro-thermographic methods are presented together with a comparison of measurement methods used to develop J_R curves and to determine crack initiation values. The reliability and accuracy of the results of each of these methods is a necessary requirement in order to develop a unique, that is, a geometry independent material characterization.

EXPERIMENTAL PROCEDURE

Equipment

An computer interactive testing system was used for the fracture toughness measurements. The unloading compliance method was used on single specimens to determine crack growth resistance curves based on the J-integral concept (J_I versus Δa_p curves) for aluminum alloys (Voss et al., 1985).

The system consisted of a microcomputer, a servohydraulic testing machine, a data acquisition/control unit, a digital multimeter, and several auxiliary devices for real time data acquisition as well as for data storage. A thermographic system was used to measure infrared emissions at the crack tip during fracture toughness testing.

Specimens

The test specimens were standard 15.5 mm (0.610 in) thick, 31.7 mm (1.28 in) wide three-point-bend, T(B), and 12.1 mm (0.5 in) thick, 31.1 mm (1.28 in) wide compact tension specimens (CTS), both taken from the ASTM TL orientation in the plate. A notch was machined in the specimen to a depth of 15.9 mm (0.628 in). To measure the crack opening displacement, an opening, 4.1 mm (0.16 in) wide by 3.0 mm (0.12 in) in depth was machined in the specimen, to which knife edges which were attached. The specimens were then fatigue precracked to an initial crack length of about 18.0 mm (0.71 in).

Two groups of specimens were tested. One group contained side grooves 1 mm deep on each side, while the other group of specimens were not side grooved.

The latter group of specimens were used for the thermography observations.

Potential Drop Measurement

In the DC potential drop measurements, four arbitrarily chosen currents (10, 20, 30, and 50 amp) were used in the calibration. The calibration consisted of machining increasing "crack lengths" into a single specimen, and measuring the change in voltage as a function of the applied current. A family of curves of voltage versus crack length for each applied current was then developed.

The test specimens were electrically insulated from the loading fixtures and clip gauge. An ohmmeter was used to monitor the resistivity changes in the specimen by measuring the DC potential drop over the crack (Bakker, 1985). The DCPD technique was found to be insensitive to external disturbances, and DC potential changes in the range of 1 μV were repeatably detected.

Infrared Emission Measurement

IR thermography has been used to measure surface IR emission distribution in metals under tensile and cyclic loading.(6,7) The experimental apparatus of an infrared camera which relays data to a black and white monitor and a control unit. The display on the monitor can be photographed and then stored on video tape so that a permanent record of results can be retained. The distance from the specimen surface and IR camera was approximately 120 mm. It was experimentally found that the signal was not dependent on the angle of obliqueness (when $\theta < \pm$ 50 deg). In order to increase the emissivity of the specimen surface to about 0.9, an infrared transparent coating was applied.

EXPERIMENTAL RESULTS

Multi-specimen Results

Twelve three-point bend specimens were tested to produce various levels of crack extension. The crack lengths are given in Table 1. Figure 1 shows a typical load-CMOD curve with partial unloadings for a fatigue precracked specimen. For these specimens, the J-integral was evaluated from the area under the load-LLD curve using the relationship (Faucher et al., 1985).

$$J = 2A/(B_N * b_o) \tag{1}$$

The tearing modulus,was evaluated using the slope of the (J versus Δa_p curve)

$$T = E * (dJ/da)/\sigma_y{}^2 \tag{2}$$

The plastic part of LLD, L_p, can be related to the plastic part of CMOD, Vp, via a plastic rotational factor, r_p,

$$Vp = L_p*(r_p*(1 - a/W) + a/W + z*W) \tag{3}$$

For these tests, the knife edge thickness, i.e. z was taken as 0, and r_p was measured and found to be 1.04.

Table 1. Measured initial, a_o, and final, a_f, crack lengths, and areas A under the load-LLD curves

Specimen	a_o (mm)	a_f (mm)	Δa_p (mm)	A (J)	A_p (J)	J (KJ/m²)
T-1	18.62	18.87	0.25	13.08	12.64	127.2
T-4	17.95	18.30	0.35	15.20	14.45	141.5
T-6	18.59	19.00	0.41	16.29	15.72	158.5
T-7	18.40	19.31	0.91	31.66	30.12	301.4
T-5	18.82	19.65	0.83	24.12	23.35	239.0
T-14	18.59	19.43	0.85	24.21	23.47	236.2
*T-8	18.39	18.78	0.39	9.33	8.91	124.9
*T-9	18.68	19.29	0.61	15.97	15.46	202.1
*T-11	18.64	19.36	0.72	14.75	14.33	193.5
*T-10	18.71	19.90	1.19	21.39	20.90	271.4
*T-2	18.47	21.20	2.73	27.83	27.39	363.8
*T-3	18.71	20.76	2.05	18.90	18.51	298.5

* These specimens had 12.5% side grooves machined into each side.

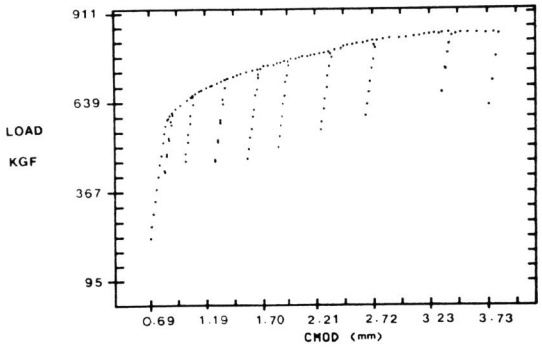

Fig. 1. Typical load-CMOD curve for fatigue pre-cracked specimen.

According to ASTM E 813, the J-integral is composed of the elastic and plastic components, J_e and J_p, which are defined as follows.

$$J_e = K^2*(1 - \mu^2)/E$$
$$J_p = 2A_p/(B_N * b_o) \text{ then}$$

$$J = J_e + J_p = K^2*(1 - \mu^2)/E + 2A_p/(B_N * b_o) \quad (4)$$

where the stress intensity factor K was calculated according to the ASTM Specification E 399, and μ is Poisson's ratio. The plastic part of the area under the load-LLD curve, A_p, was evaluated by means of the trapezoidal rule using the CMOD, and equation 3.

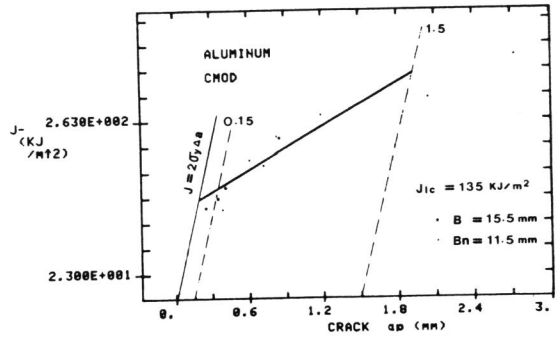

Fig. 2. J-Resistance curve for aluminum T(B) specimens.

Using the crack length results given in Table 1, the J vs Δa_p curve was plotted and is shown in Fig. 2. J_{IC} was found to be 135 KJ/m², and the tearing modulus T, 9.9.

Partial Unloading Compliance Method, or Single Specimen Method

Instead of using the multiple specimen technique, the growing crack length can also be determined from measurements of the elastic compliance of a single specimen. Both methods also give the crack length value at each partial unloading point along the load-displacement curve. The J-integral was evaluated using equation 4. A more accurate method for determining J, taking crack extension into account is made using the following:

$$J_i = J_{ei} + J_{pi} \quad (5)$$

where

$$J_{ei} = (K_i^2 * (1 - \mu^2))/E \quad (6)$$

and

$$J_{pi} = (J_{pi-1} + n_i * A_{i,i-1}/B_N * b_i) * (1 - \gamma_i(a_i - a_{i-1})/b_i) \quad (7)$$

Where the $n_i = 2$, and $\gamma_i = 1$ for T(B) specimen, the index i refers to the appropriate value at the i-th unloading cycle, and $A_{i,i-1}$ is the area A (or A_p) between unloadings i and i-1. The original precracked length, a_o, was located on the blunting line. The i-th crack extension a_i was corrected to be on the blunting line, such that:

$$a_i = a_o + J_{pi}/2\sigma_y \quad (8)$$

All crack lengths are finally adjusted to the measured initial crack length by adding to their value the difference between the calculated and measured initial crack length.

The J vs Δa_p curves obtained for each specimen are plotted in Fig. 3 using values calculated from CMOD data.

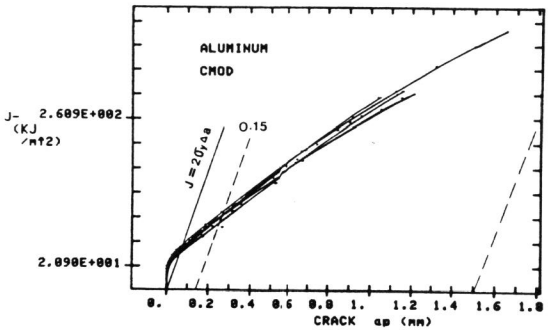

Fig. 3. J-Resistance curves for each specimen obtained from CMOD measurements.

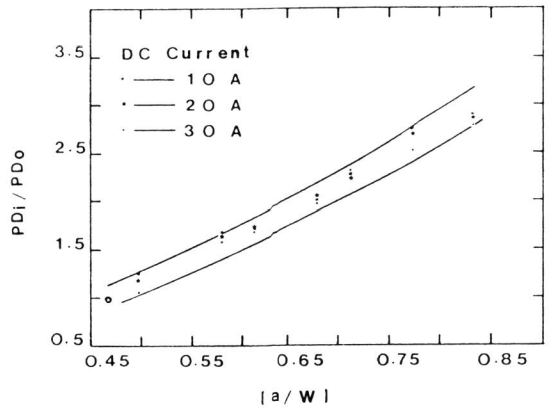

Fig. 4. DCPD calibration curves for CT specimen.

DC Potential Difference Analysis

Compact tension specimens were used to generate a DC potential drop calibration curve. The data was generated by saw cutting a number of cracks to various length and recording the corresponding potentials at those crack lengths. Calibrations were performed at the arbitrarily chosen input currents of 10, 20, 30 amperes. The crack lengths and DCPD values are given in Table 2 and the representative curve is shown in Fig. 4.

When DC flows through the test specimen, the temperature near the crack tip rises quickly. This temperature rise causes the change in thermoelectric potential at the measuring points on the specimen. The temperature changes at the crack tip with various crack lengths. Their corresponding DCPD values for the input currents of 10, 20, 30 amperes are shown in Table 2. The crack lengths ranged from an a_0 of 11.93 mm to an a_7 of 21.16 mm.

It is clear from experimental observations that the effect of the thermoelectric potential must be included in the measurement of the DC

Table 2. Crack lengths of CT specimens and corresponding DCPD values.

Crack length (mm)		10 (amp) PD_i/PD_o	20 (amp) PD_i/PD_o	30 (amp) PD_i/PD_o	Crack growth $\Delta a = a_i - a_o$
a_o	11.93	1.00	1.00	1.00	0
a_1	12.66	1.28	1.19	1.13	0.73
a_2	14.73	1.70	1.63	1.60	2.80
a_3	15.50	1.74	1.71	1.69	3.57
a_4	17.23	2.09	2.05	1.97	5.30
a_5	18.10	2.22	2.27	2.33	6.17
a_6	19.59	2.71	2.79	2.45	7.66
a_7	21.16	2.86	2.87	2.76	9.23

potential drop. For when larger DC currents were passed through the test specimen, the effect of thermoelectric potential was found to be much higher. When the DC potential method is used, if the test specimen is allowed to stabilize for at least 20 minutes before taking a reading, the measured error can be reduced as much to less than 2%.

Initial DCPD experiments conducted on three - point bend specimens that were fatigued, indicated that a measurement sensitivity of 7.4 μV/mm could be attained in the determination of the crack length. Using the DCPD apparatus a calibration specimen was fatigued to a certain crack length. Tensile loading was applied immediately after the fatigue precracking, i.e. straining without interruption from the mean level of the test fatigue load cycle in order to mark the end of the fatigue crack. Additional fatiguing was conducted, and the tensile loading needed to mark the end of the fatiguing repeated. Once a number of fatigue cracks were grown, the specimen was fractured and every fatigue crack length was measured using the nine point technique. The results in the form of a continuously increasing DCPD signal are shown in Fig. 5.

The DCPD is expressed as a function of crack length a_i in the form:

$$PD_i/PD_o = 2.06 - 0.16 * a_i + 0.006 * a_i^2 \qquad (9)$$

Figure 6 shows a plot of the load/CMOD and DCPD/CMOD curves. The DCPD for the bend specimen did not show a discontinuity at crack extension, Q in Fig. 6, but a significant slope change can be seen at about 1.1 mm crack extension. However, the test did not show any clear correlation between the DC potential change and crack initiation. In Fig. 6 the DCPD data for larger crack extensions were within acceptance limits of the ASTM Test for J_{IC}, 15%. The relatively large error found at low Δa_p values was due to the plasticity effects that were produced by local thickness reductions of up to 12%.

IR Emission Measurements at Crack Tip

Recent work indicates that the IR thermographic technique has the ability to measure crack length during loading (Stanley et. al. 1986 and Huang et. al, 1987). This technique depends on the IR cooling emission (IRCE) and IR heating emission (IRHE) of metals during deformation. In this phase of the work, the unloading compliance method and real time vibro-thermographic technique were used to determine the crack length.

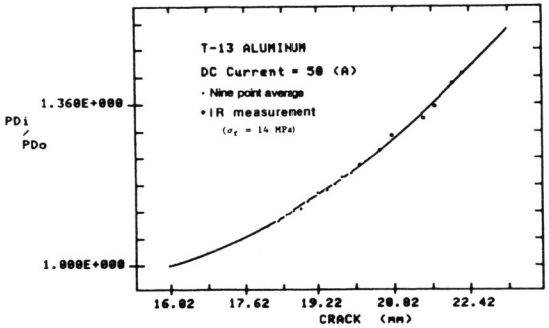

Fig. 5. DCPD curve obtained for the T(B) fatigue cracked specimens.

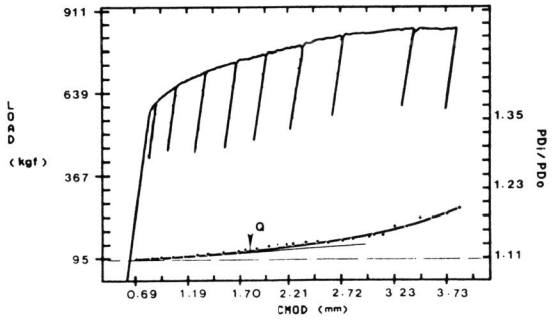

Fig. 6. Load- CMOD and DCPD CMOD curves.

The objective of this investigation was to develop a thermographic technique for the measurement of crack extension in three - point bend specimens taken from the LT orientation in the plate, and employ this technique in the determination of the J - R curve for the 5052 -H112 aluminum alloy. This type of aluminum is used in the manufacture of tank cars that carry hazardous materials. The results of a calibration of infrared crack position are shown in Table 3.

After each unloading, the IRCE and IRHE were found to be concentrated in the area of crack tip, extending radially at 45 deg, and along the crack front.

The video records clearly showed a continuous IR emission process- alternating crack tip blunting and ductile crack extension. This was observed from the very beginning of the fracture toughness test up to the largest applied crack extension, i.e. at failure. Infrared images of the crack tip at the beginning and the end of a fracture toughness test show that the blunting area is concentrated near the crack tip, and there was no evidence of crack extension. Once the CMOD increased to 8.1 mm, the crack extension was found using the IR images.

Upon loading, the CMOD changed significantly from 7.4 mm to 8.9 mm, but the crack tip optical phenomena remained the same. The Δa_p values were measured along the IRCE and IRHE areas on the specimen's surface.

Table 3. Comparisons of crack lengths measured using optical and thermographic techniques.

	Crack length (mm)		Different (mm)	Measured error (%)		
	Optical	Infrared	$\Delta L = L_o - L_I$	Y_o	Y_I	Y_{o-I}
a_o	11.93	11.82	+0.11	1.4	1.7	1.0
a_1	12.66	12.84	-0.18	1.8	1.5	-1.4
a_2	14.37	14.25	+0.12	0.1	2.2	3.3
a_3	15.50	15.50	+0.00	1.5	1.3	0
a_4	17.23	17.63	+0.40	1.7	0.7	-2.2
a_5	18.10	18.42	-0.32	0.1	0.5	-1.7
a_6	15.59	20.07	-0.48	1.3	0.1	-2.4
a_7	21.16	21.18	-0.02	1.5	0.1	0.1

Comparison of PUC, DCPD, and IR Methods

Because it is difficult to establish the accuracy of each method, it is important to have a good concept of the approximations made and of the advantages and limitations of each method. Figure 7 shows the results obtained from a partial unloading compliance experiment plotted with the corresponding measurement of both the DC potential drop and IR crack extension. For this comparison, the calibration curves for both the DCPD and IR methods were adjusted to the crack lengths measured at the ninth unloading compliance test value, using the same specimen (T-14). The J vs Δa_p curves, Fig. 8, for this specimen were found to be in good agreement with each other. The final crack lengths using each method were measured and Δa_p values of 1.18 (mm) for (PUC), 1.12 mm for (DCPD), and 1.43 mm for (IR) were found. The differences between the values obtained using these three methods provide toughness values which are within the ASTM acceptance limit of 15% for J_{IC} .

The results obtained using the DCPD method with those obtained using the IR method are shown in Figs. 6 and 7. The DCPD technique does not differentiate between crack tip plasticity and crack extension. Proper application of this technique depends on a continuously increasing DCPD signal, and we have found that a minimum in the DCPD signal, sometimes interpreted as the moment of crack initiation, was not observed. At low Δa_p values, the DCPD data over estimated the crack length because of the relatively large contribution, more than 15%, produced by the plasticity. The main difficulty associated with using either the PUC or the DCPD method is the determination of crack length in the early stages of the test.

The crack initiation is defined at point Q of the measured IR crack extension curve shown in Fig. 7. This point occurs at a lower CMOD than that found using the DCPD method, and it represents an accurate IR image of the beginning of the crack extension.

A disadvantage of the unloading compliance and vibro-thermographic method comes from repeated interruptions, i.e. unloadings, during the test. Although partial unloadings and un-damaging fatigue loadings should not affect material properties, they certainly cannot be carried out at high rates of loading.

CONCLUSIONS

Different procedures can be used to determine the amount of crack growth

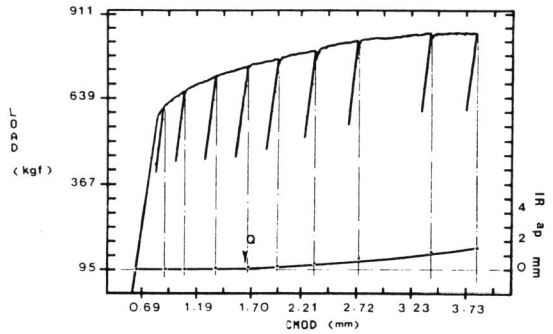

Fig. 7. Load-deflection diagram with corresponding IR crack extension.

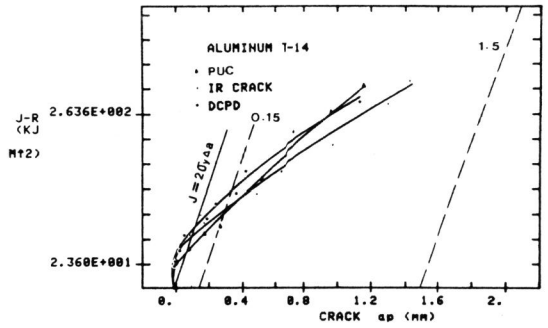

Fig. 8. J vs Δa_p curves evaluated using Figs. 6 and 7.

used to determine the material parameter J_{IC}, and J crack growth resistance curves for the characterization of crack initiation and stable crack growth.

The DC potential drop method allows for the evaluation of a continuous $J_R(\Delta a_p)$ curve if the initiation of crack is given. There remains some uncertainty with this point of initiation because the physical sources of the change of potential under loading are not well understood.

Vibro-thermographic technique provide good estimates of crack extension and real-time records of the continuous test process. Used with common unloading compliance methods, they give the full J-resistance curve. The J_{IC} value of the material tested was found to be 135 KJ/m^2, or 781.4 in-lbs/in^2. This corresponds to a fracure toughness, K, of 160.5 Ksi (in)†½.

ACKNOWLEDGMENTS

The help of Dr. R. deWit, Mr. S.R. Low III, and Mr. C.H. Brady of the Metallurgy Division in the experimental phase is gratefully acknowledged. Also, the help of Dr. R. Grot of National Engineering Laboratory of NBS, and the use of his infrared equipment is gratefully appreciated.

REFERENCES

ASTM E-813 (1987). "Standard Test Method for J_{IC}, A MEASURE OF FRACTURE TOUGHNESS, American Society for Testing and Materials, pp.968-990.

Bakker, A. (1985). "A DC Potential Drop Procedure for Crack Initiation and R-Curve Measurements During Ductile Fracture Tests," Elastic-Plastic Fracture Test Methods: The User's Experience, ASTM STP-856, E.T. Wessel and F.J. Loss Eds. American Society for Testing and Materials, pp. 394-410.

Charles, J.A., Appl F.F., and Francies, J.E. (1978). "Using the Scanning Infrared Camera in Experimental Fatigue Studies," Transaction of the ASME, Vol. 100, p. 200-204.

Faucher, B, and Tyson, W.R. (1985). "Measurements of J-Resistance Curves with Three Point Bend Specimens," The Mechanism of Fracture, Conference proceedings, ASM, V.S. Loss Editor, pp. 205-214.

Hackett, E.M. and Vassilaros, M.G. (1983). "J-Integral R-Curve Testing of HY Steels Utilizing the D.C. Potential Drop Method," Naval Sea Systems Command (SEA 05R), Washington, D.C. 20362.

Huang, Y., Hicho, G.E. and Fields, R.J. (1987). "Infrared Measurements of Heating and Cooling Emissions in Aluminum and Steel During Tensile and Cyclic Loading," NBSIR 87-3653.

Huang, Y. and Shih C.H. (1985). "Application of Infrared Technique in Research of Mechanical Properties," International Centre for Theoretical Physics, Technical Report, IC/85/180, Italy.

Joyce, J.A. and Schneider, C.S. (1986). "Application of Alternating Current Potential Difference to Crack Length Measurement During Rapid Loading," U.S. Naval Academy, Annapolis, MD 21402.

Stanley, P. and Chan, W.K. (1986). "SPATE Stress Studies of Plates and Rings Under In-Plane Loading," Experimental Mechanics, De, pp. 360-370.

Voss, B. and Mayville, R.A. (1985). "The Use of the Partial Unloading Compliance Method for the Determination of J-R Curves and JI_C Elastic-Plastic Fracture Test Methods," STP 856, American Society for Testing and Materials, Philadelphia, PA, pp. 117-130.